Hyperspectral Image Restoration by Tensor Fibered Rank Constrained Optimization and Plug-and-Play Regularization

Yun-Yang Liu[1]

Xi-Le Zhao[1], Yu-Bang Zheng[1], Tian-Hui Ma[2], Hongyan Zhang[3]

[1]University of Electronic Science and Technology of China

[2]Civil Aviation University of China

[3]Wuhan University

9 Oct 2021

Outline

Hyperspectral Image (HSI)

HSIs contain wealthy spatial-spectral knowledge and have been widely used in many applications, such as material identification, mineral detection, and forest inspection.

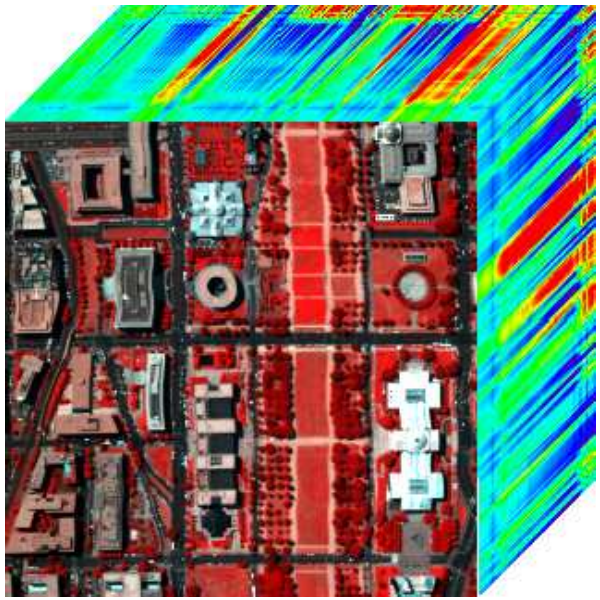

Why Study HSI Denoising?

Due to the limitation of imaging conditions, HSIs are inevitably contaminated by various kinds of noise, e.g., Gaussian noise, impulse noise, stripes, and deadlines, which degrades the HSIs quality and limits the subsequent applications.

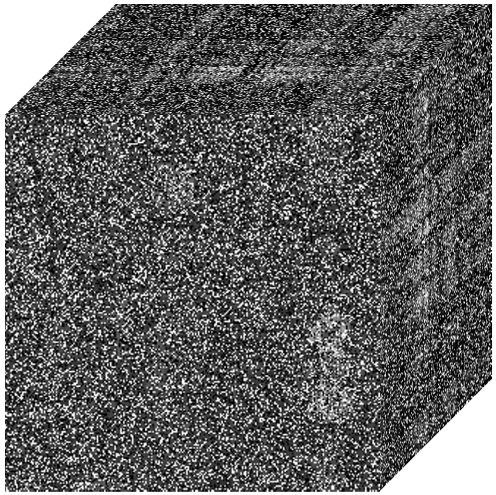

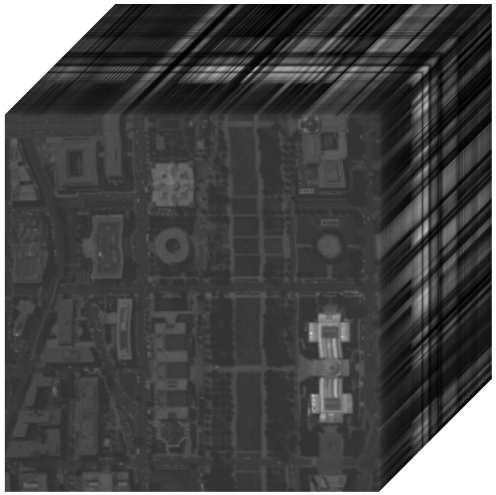

Conclusive Issue for HSI Denoising

Exploring accurate spatial-spectral prior knowledge of HSIs:

- piecewise smoothness;
- nonlocal self-similarity;
- low-rankness;
- . . .

Tensor

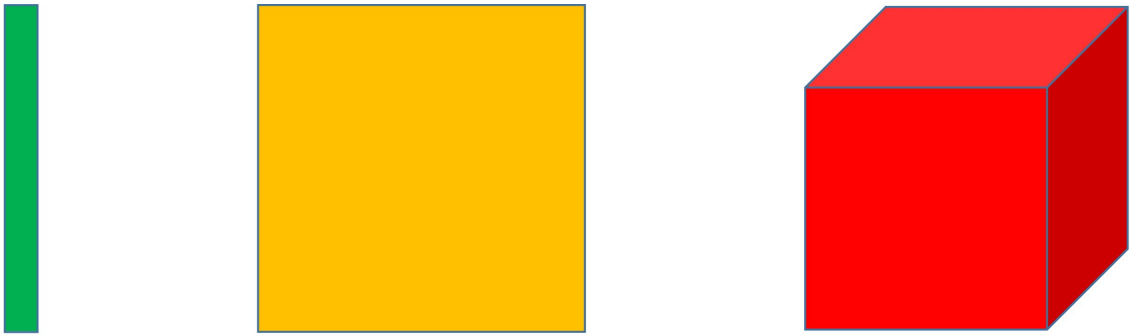

Tensor Basics (Fibers and Slices)

A *fiber* of a tensor $\mathcal{X}$ is a vector generated by fixing every index but one.

A *slice* of a tensor $\mathcal{X}$ is a matrix generated by fixing every index but two.

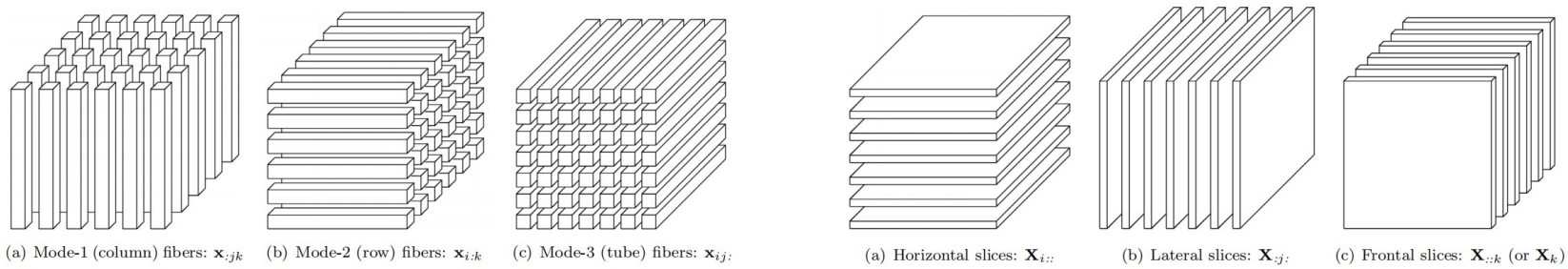

Figure 1: Fibers and slices of three-way tensors.

T-Product and T-SVD

T-product: $\mathcal{F} = \mathcal{X} * \mathcal{Y} \Leftrightarrow \mathcal{F}(i,j,:) = \sum_{t=1}^{n_2} \mathcal{X}(i,t,:) \star \mathcal{Y}(t,j,:)$, where $\star$ denotes the circular convolution between two tubes.

T-Product and T-SVD

T-product: $\mathcal{F} = \mathcal{X} * \mathcal{Y} \Leftrightarrow \mathcal{F}(i,j,:) = \sum_{t=1}^{n_2} \mathcal{X}(i,t,:) \star \mathcal{Y}(t,j,:)$, where $\star$ denotes the circular convolution between two tubes.

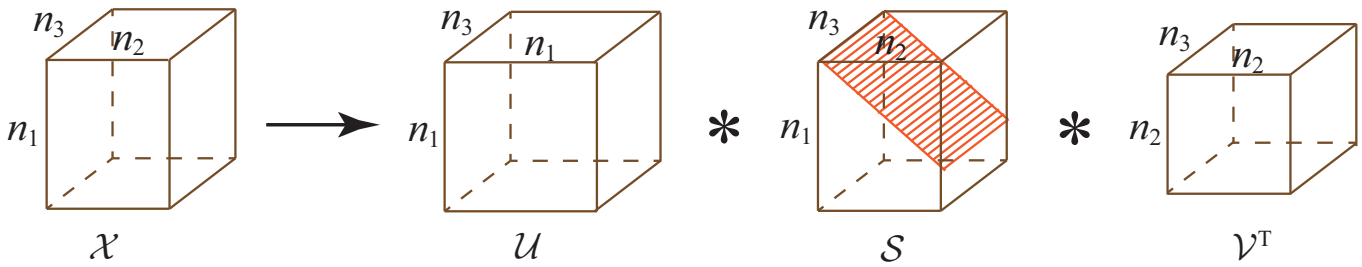

Figure 2: The t-SVD for third-order tensor.

[1] M. E. Kilmer and C. D. Martin, Factorization Strategies for Third-order Tensors, **LAA**, 2011.

Tubal Rank and TNN

The tubal rank of $\mathcal{X}$ is defined as the number of non-zero tubes of $\mathcal{S}$, i.e.,

$$\text{rank}_t(\mathcal{X}) := \#\{i : \mathcal{S}(i,i,:) \neq 0\}.$$

Tubal Rank and TNN

The tubal rank of $\mathcal{X}$ is defined as the number of non-zero tubes of $\mathcal{S}$, i.e.,

$$\text{rank}_t(\mathcal{X}) := \#\{i : \mathcal{S}(i,i,:) \neq 0\}.$$

The tensor nuclear norm (TNN) of $\mathcal{X}$ can be computed via the summation of the matrix nuclear norm of Fourier transformed frontal slices , i.e.,

$$\|\mathcal{X}\|_{\text{TNN}} = \sum_{i=1}^{n_3} \|\bar{X}^{(i)}\|_*,$$

where $\bar{X}^{(i)}$ is the i-th frontal slice of $\bar{\mathcal{X}}$ with $\bar{\mathcal{X}} = \texttt{fft}(\mathcal{X}, [], 3)$.

[2] Z. M. Zhang *et al*., Novel Methods for Multilinear Data Completion and De-noising Based on Tensor-SVD, **CVPR**, 2014.

Illustration

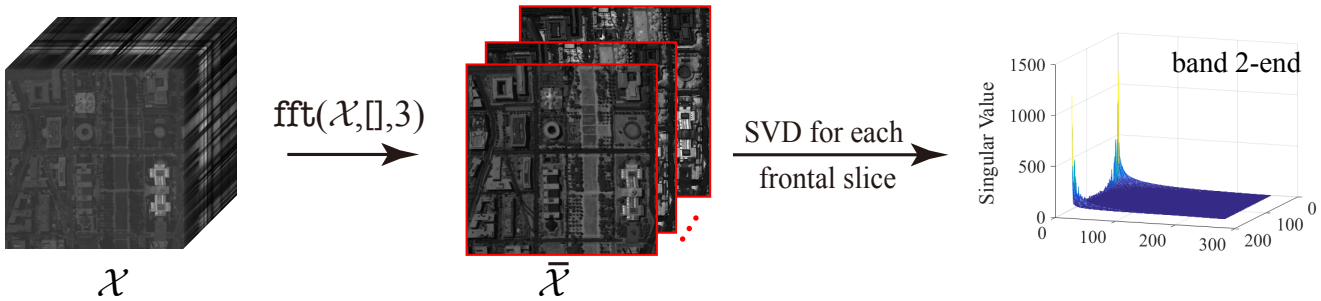

Figure 3: The t-SVD for an HSI.

When setting the band of an HSI to be the frontal slice of a three-way tensor, the t-SVD characterizes its spatial correlations via SVDs, while describes its spectral correlation by the embedded circular convolution or DFT.

Mode-k T-Product

Mode-k t-product ($*_k$):

$$\mathcal{F} = \mathcal{X} *_1 \mathcal{Y} \Leftrightarrow \mathcal{F}(:,j,s) = \sum_{t=1}^{n_3} \mathcal{X}(:,j,t) \star \mathcal{Y}(:,t,s),$$

$$\mathcal{F} = \mathcal{X} *_2 \mathcal{Y} \Leftrightarrow \mathcal{F}(i,:,s) = \sum_{t=1}^{n_1} \mathcal{X}(t,:,s) \star \mathcal{Y}(i,:,t),$$

$$\mathcal{F} = \mathcal{X} *_3 \mathcal{Y} \Leftrightarrow \mathcal{F}(i,j,:) = \sum_{t=1}^{n_2} \mathcal{X}(i,t,:) \star \mathcal{Y}(t,j,:).$$

[3] Y.-B. Zheng *et al*., Mixed Noise Removal in Hyperspectral Image via Low-fibered-rank Regularization, **TGRS**, 2020.

Mode-*k* T-SVD and Fibered Rank

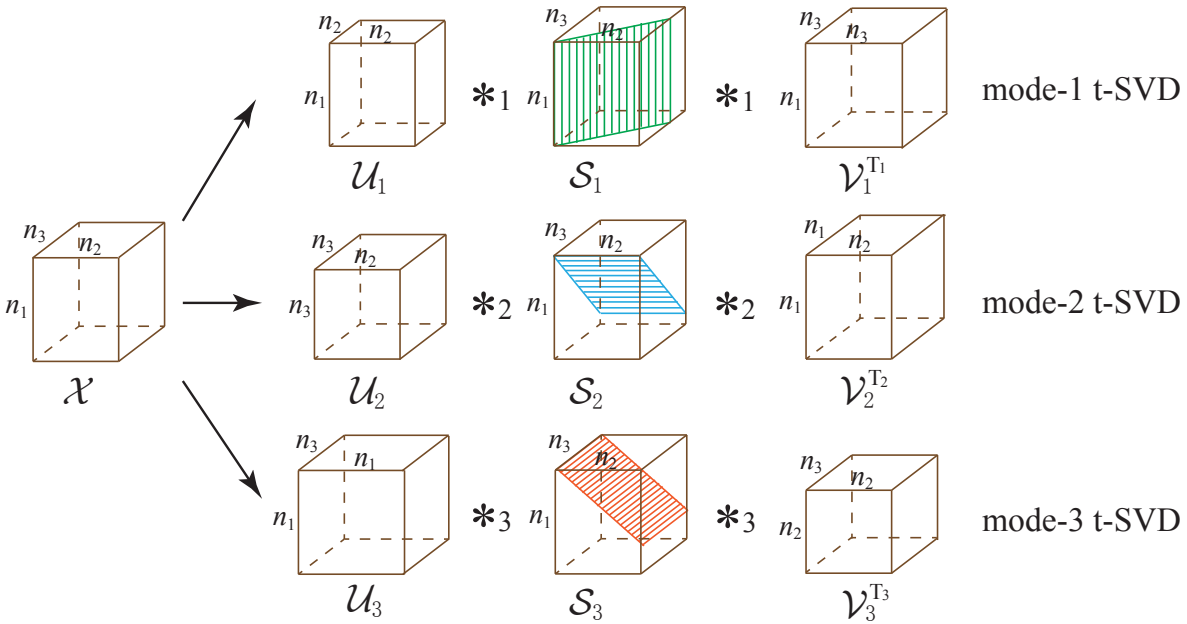

Figure 4: The mode-*k* t-SVD for three-way tensors (*k*=1,2,3).

Mode-*k* T-SVD and Fibered Rank

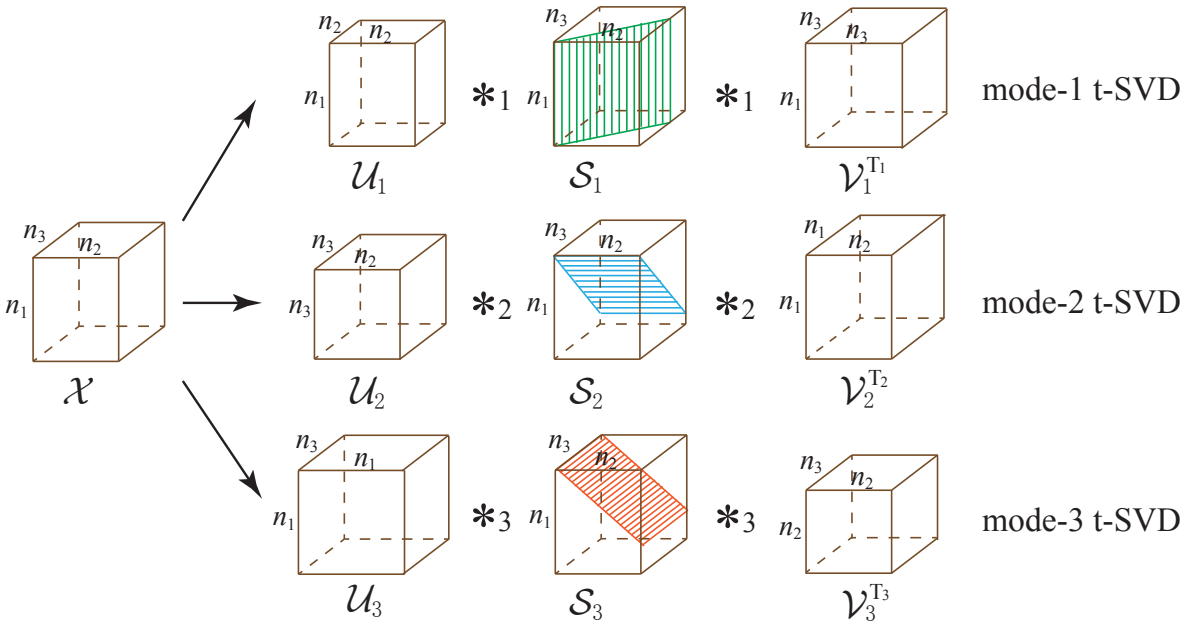

Figure 4: The mode-*k* t-SVD for three-way tensors (*k*=1,2,3).

The mode-*k* fibered rank: $\mathrm{rank}_{\mathrm{f}_k}(\mathcal{X})$ is defined as the number of non-zero mode-*k* fibers of $\mathcal{S}_k$.

Mode-*k* T-SVD and Fibered Rank

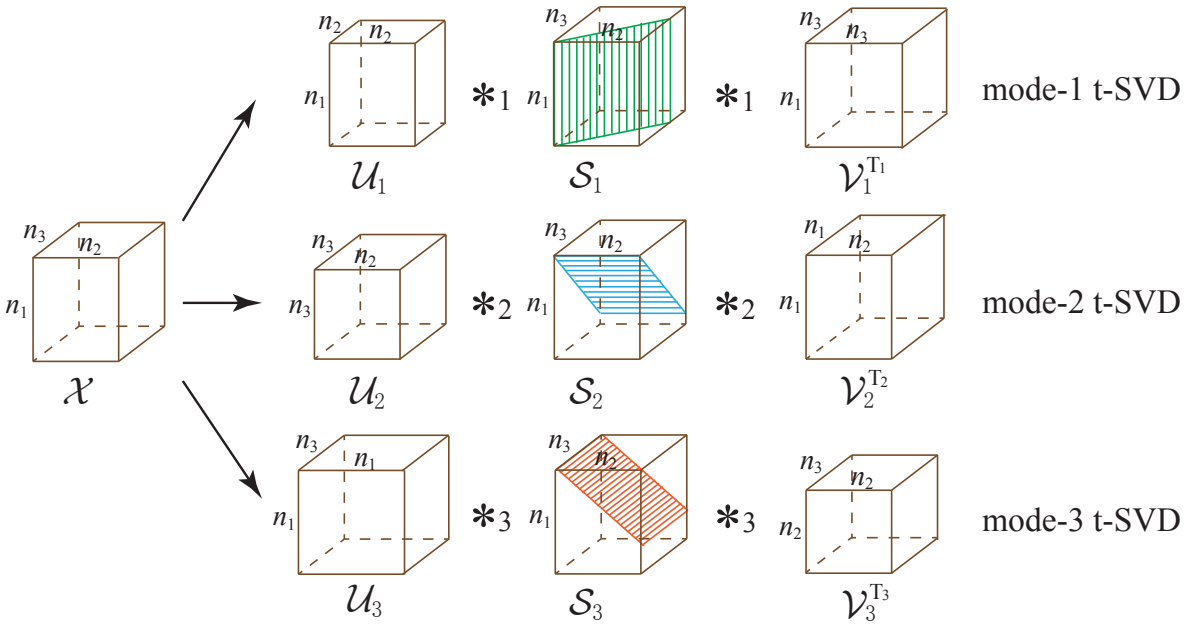

Figure 4: The mode-*k* t-SVD for three-way tensors (*k*=1,2,3).

The mode-*k* fibered rank: $\mathrm{rank}_{\mathrm{f}_k}(\mathcal{X})$ is defined as the number of non-zero mode-*k* fibers of $\mathcal{S}_k$.

The fibered rank: $\mathrm{rank}_{\mathrm{f}}(\mathcal{X}) = \left(\mathrm{rank}_{\mathrm{f}_1}(\mathcal{X}), \mathrm{rank}_{\mathrm{f}_2}(\mathcal{X}), \mathrm{rank}_{\mathrm{f}_3}(\mathcal{X})\right)$.

Low-Fibered-Rank Prior for An HSI

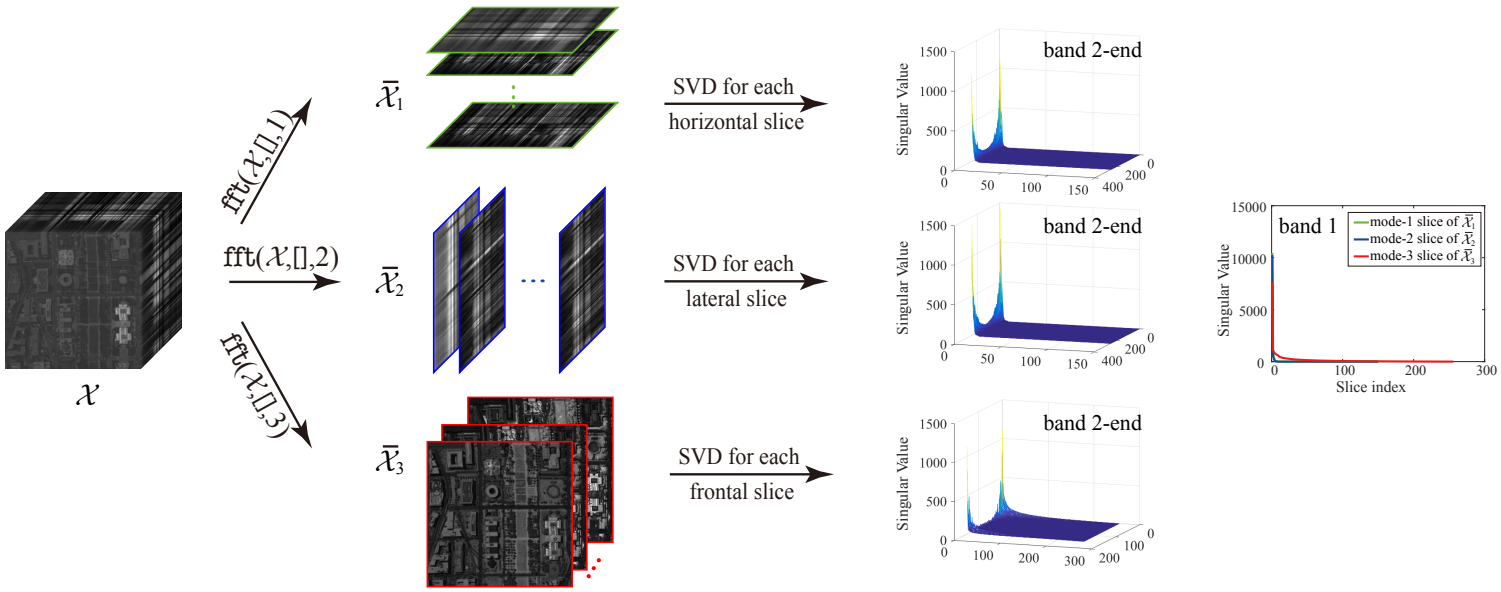

Figure 5: The mode-k t-SVD for an HSI.

Low-Fibered-Rank Prior for An HSI

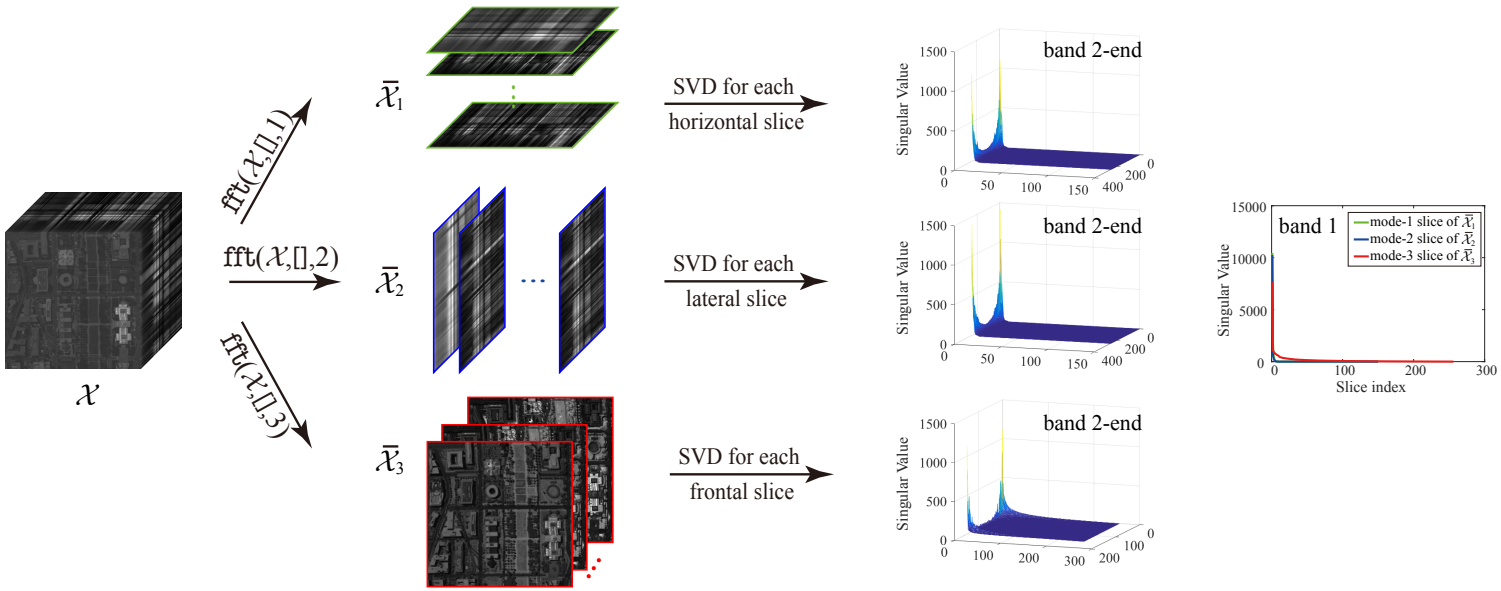

Figure 5: The mode-k t-SVD for an HSI.

Table 1: The rank estimation of an HSI.

Data	Size	Tucker rank	Tubal rank	Fibered rank
Washington DC Mall	$256 \times 256 \times 150$	(107,110,6)	182	(8,8,182)

Convex Relaxation: Three-Directional Tensor Nuclear Norm (3DTNN)

Mode-k TNN: $\|\mathcal{X}\|_{\text{TNN}_k}$ is defined as the sum of singular values of all the mode-k slices of $\bar{\mathcal{X}}_k$, i.e.,

$$\|\mathcal{X}\|_{\text{TNN}_k} := \sum_{i=1}^{n_k} \left\|(\bar{X}_k)_k^{(i)}\right\|_*,$$

where $(\bar{X}_k)_k^{(i)}$ is the i-th mode-k slice of $\bar{\mathcal{X}}_k$ with $\bar{\mathcal{X}}_k = \texttt{fft}(\mathcal{X}, [], k)$.

Convex Relaxation: Three-Directional Tensor Nuclear Norm (3DTNN)

Mode-k TNN: $\|\mathcal{X}\|_{\text{TNN}_k}$ is defined as the sum of singular values of all the mode-k slices of $\bar{\mathcal{X}}_k$, i.e.,

$$\|\mathcal{X}\|_{\text{TNN}_k} := \sum_{i=1}^{n_k} \|(\bar{X}_k)_k^{(i)}\|_*,$$

where $(\bar{X}_k)_k^{(i)}$ is the i-th mode-k slice of $\bar{\mathcal{X}}_k$ with $\bar{\mathcal{X}}_k = \texttt{fft}(\mathcal{X}, [], k)$.

3DTNN: $\|\mathcal{X}\|_{\text{3DTNN}}$ is defined as

$$\|\mathcal{X}\|_{\text{3DTNN}} := \sum_{k=1}^{3} \alpha_k \|\mathcal{X}\|_{\text{TNN}_k},$$

where $\alpha_k \geq 0$ $(k = 1, 2, 3)$ and $\sum_{k=1}^{3} \alpha_k = 1$.

3DTNN-Based HSI Denoising Model

Considering a target HSI $\mathcal{X} \in \mathbb{R}^{n_1 \times n_2 \times n_3}$, the proposed 3DTNN-based HSI denoising model is formulated as

$$\begin{aligned} \min_{\mathcal{X},\mathcal{N},\mathcal{S}} \ & \|\mathcal{X}\|_{\text{3DTNN}} + \lambda_1 \|\mathcal{N}\|_F^2 + \lambda_2 \|\mathcal{S}\|_1, \\ \text{s.t.} \ & \mathcal{Y} = \mathcal{X} + \mathcal{N} + \mathcal{S}, \end{aligned} \tag{1}$$

where $\mathcal{Y}$ is the observed HSI, $\mathcal{N}$ is Gaussian noise, and $\mathcal{S}$ is sparse noise.

Motivation

The convex and non-convex surrogates **cannot well approximate** the singular values and singular vectors of slices after the Fourier transform. **We directly constrain the tensor fibered rank (FRCTR) of the solution.**

Motivation

The convex and non-convex surrogates **cannot well approximate** the singular values and singular vectors of slices after the Fourier transform. **We directly constrain the tensor fibered rank (FRCTR) of the solution.**

Only considering the low-rankness prior usually **faces limitations** in preserving local details and removing the noise with low-rank property, such as stripe noise and deadlines. **We introduce an implicit regularizer under the Plug-and-Play (PnP) framework.**

The PnP-based framework for HSI restoration.

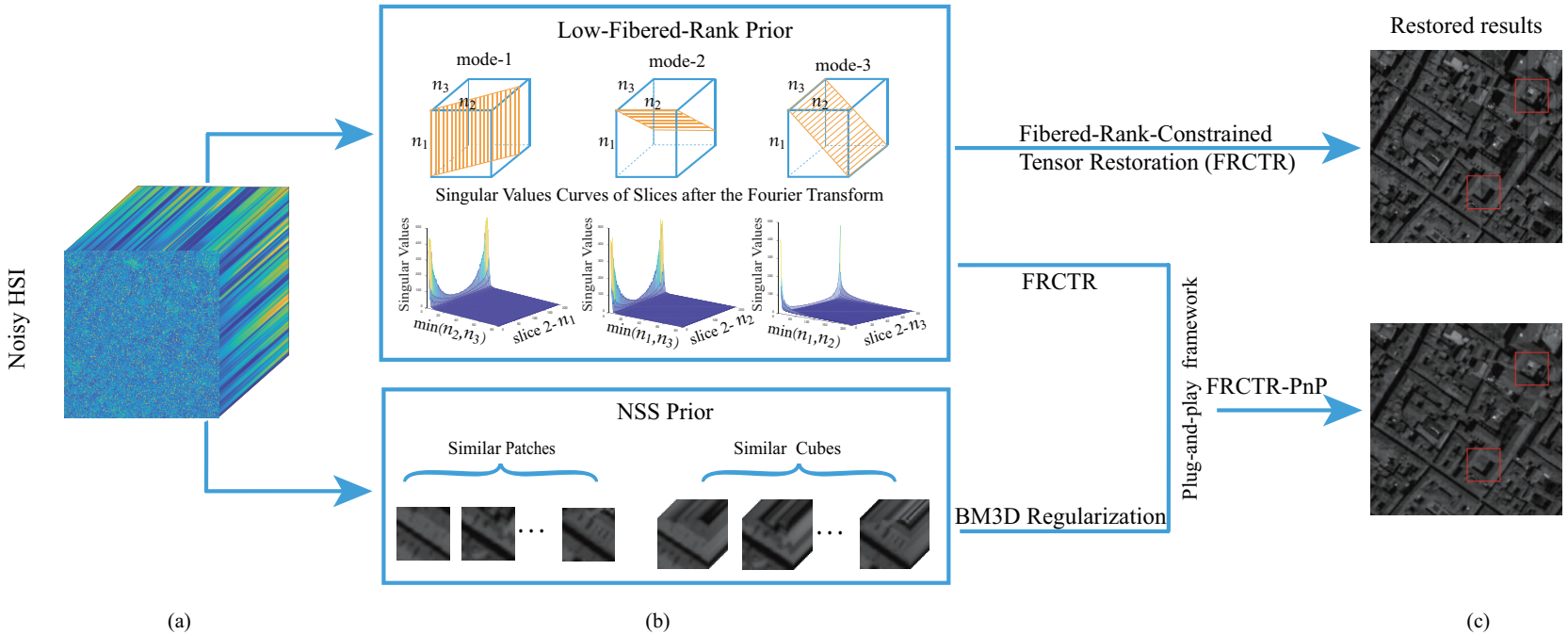

Figure 6: The PnP-based framework for HSI restoration. (a) A noisy HSI. (b) Illustration of low-fibered-rank prior and nonlocal self-similarity prior. (c) The restored results of the simulated experiment.

Outline

FRCTR-PnP model for HSI denoising

We suggest a novel HSI restoration model by introducing a FRCTR with an embedded PnP-based regularization (FRCTR-PnP) as

$$\begin{aligned} &\min_{\mathcal{X},\mathcal{S}} \|\mathcal{S}\|_1 + \lambda\Phi(\mathcal{X}) \\ &\text{s.t. } \|\mathcal{Y}-\mathcal{X}-\mathcal{S}\|_F^2 \le \epsilon, \text{rank}_{\text{f}}(\mathcal{X}) \le [r_1, r_2, r_3], \end{aligned} \tag{2}$$

where $\mathcal{Y}$ denotes the observed HSI, $\mathcal{S}$ denotes sparse noise, $[r_1, r_2, r_3]$ is the upper bound of the fibered rank of $\mathcal{X}$, and $\Phi(\mathcal{X})$ is an implicit regularizer exploiting certain priors of the HSI.

ADMM-Based Algorithm

We develop an ADMM-based algorithm to solve (2). By introducing auxiliary variables $\mathcal{F}_k$ $(k = 1, 2, 3)$ and $\mathcal{L}$, (2) can be rewritten as

ADMM-Based Algorithm

We develop an ADMM-based algorithm to solve (2). By introducing auxiliary variables $\mathcal{F}_k$ $(k = 1, 2, 3)$ and $\mathcal{L}$, (2) can be rewritten as

$$\begin{aligned} &\min_{\mathcal{X},\mathcal{S},\mathcal{F}_k} \|\mathcal{S}\|_1 + \lambda\Phi(\mathcal{L}) \\ &\quad \text{s.t. } \|\mathcal{Y} - \mathcal{X} - \mathcal{S}\|_F^2 \le \epsilon, \mathcal{X} = \mathcal{L}, \\ &\qquad \mathcal{X} = \mathcal{F}_k, \text{rank}_{\text{f}_k}(\mathcal{F}_k) \le r_k \ (k = 1, 2, 3), \end{aligned} \tag{3}$$

The augmented Lagrangian function of (3) is

$$\begin{aligned}\mathcal{L}_{\beta_k}(\mathcal{X},\mathcal{F}_k,\mathcal{L},\mathcal{S},\mathcal{P}_k) = &\sum_{k=1}^{3}\{\langle \mathcal{X}-\mathcal{F}_k,\mathcal{P}_k\rangle + \frac{\beta_k}{2}\|\mathcal{X}-\mathcal{F}_k\|_F^2\}\\ &+ \|\mathcal{S}\|_1 + \langle \mathcal{Y}-\mathcal{X}-\mathcal{S},\mathcal{P}_4\rangle + \frac{\beta_4}{2}\|\mathcal{Y}-\mathcal{X}-\mathcal{S}\|_F^2\\ &+ \lambda\Phi(\mathcal{L}) + \langle \mathcal{X}-\mathcal{L},\mathcal{P}_5\rangle + \frac{\beta_5}{2}\|\mathcal{X}-\mathcal{L}\|_F^2\\ &\text{s.t. } \mathrm{rank}_{\mathrm{f}_k}(\mathcal{F}_k) \le r_k \ (k=1,2,3),\end{aligned}$$

ADMM-Based Algorithm

Algorithm 1 ADMM-based optimization algorithm for solving FRCTR-PnP.

Input: The noisy HSI $\mathcal{Y}$, parameter λ, fibered rank $[r_1, r_2, r_3]$, oversampling parameter $[p_1, p_2, p_3]$, stopping criteria ϵ, and acceleration parameter δ.

Initialization: $t = 0$, let $\mathcal{X}^0$, $\mathcal{S}^0$, $\mathcal{L}^0$ $\mathcal{F}_k^0$, $(k = 1, 2, 3)$ and Lagrangian multiplies $\mathcal{P}_k^0$ $(k = 1, 2, \cdots, 5)$ be zeros tensors, and parameter β_k $(k = 1, 2, \cdots, 5)$.

while not converged **do**

Update $\mathcal{F}_k^{t+1} = \text{3DRT-SVD}(\mathcal{X}^t + \mathcal{P}_k^t/\beta_k, [r_1, r_2, r_3], [p_1, p_2, p_3])$, $k = 1, 2, 3$.

Update $\mathcal{L}^{t+1} = \text{BM3D}(\mathcal{X}^t + \mathcal{P}_5^t/\beta_5, \sigma)$.

Update $\mathcal{S}^{t+1} = \text{soft}(\mathcal{Y} - \mathcal{X}^t + \mathcal{P}_4^t/\beta_4, 1/\beta_4)$.

Update $\mathcal{X}^{t+1} = \left\{ \sum_{k=1}^3 \beta_k(\mathcal{F}_k^{t+1} - \mathcal{P}_k^t/\beta_k) + \beta_4(\mathcal{Y} - \mathcal{S}^t + \mathcal{P}^4/\beta_4) + \beta_5(\mathcal{L}^{t+1} - \mathcal{P}_5^t/\beta_5) \right\} / \sum_{k=1}^5 \beta_k$.

Update $\mathcal{P}_k^{t+1} = \mathcal{P}_k^t + \beta_k(\mathcal{X} - \mathcal{F}_k^{t+1})$, $k = 1, 2, 3$.

Update $\mathcal{P}_4^{t+1} = \mathcal{P}_4^t + \beta_4(\mathcal{Y} - \mathcal{X}^{t+1} - \mathcal{S}^{t+1})$.

Update $\mathcal{P}_5^{t+1} = \mathcal{P}_5^t + \beta_5(\mathcal{X}^{t+1} - \mathcal{L}^{t+1})$.

Let $\beta_k = \min(\delta\beta_k, \beta_{\max})$; $t = t + 1$.

Check the convergence condition $\|\mathcal{X}^{t+1} - \mathcal{X}^t\|_F / \|\mathcal{X}^t\|_F < \epsilon$.

end while

Output: The restored HSI $\mathcal{X}$.

Computational Cost

Computational cost:

$$\mathcal{O}(n_1 n_2 n_3 \log(n_1 n_2 n_3) + n_1 n_2 n_3 \sum_{i=1}^{3}(r_i + p_i) + n_1 n_2 n_3).$$

Outline

Compared Methods

Compared Methods:

- wavelet-based method FORPDN [*Rasti et al., IEEE JSTARS 2014*];
- subspace-based method SNLRSF [*Cao et al., IEEE JSTARS 2019*];
- T-SVD-based method SSTV-LRTF [*Fan et al., IEEE TGRS 2018*];
- Tucker decomposition-based method LRTDTV [*Wang et al., IEEE JSTARS 2018*];
- mode-k T-SVD based method 3DTNN and 3DLogTNN [*Zheng et al., IEEE TGRS 2020*].

Simulated Experiments

Five types of noise:

- Gaussian Noise;
- Gaussian Noise + Salt and Pepper Noise;
- Gaussian Noise + Salt and Pepper Noise+ Stripe Noise;
- Gaussian Noise + Salt and Pepper Noise+ Deadlines;
- Gaussian Noise + Salt and Pepper Noise+ Stripe Noise+ deadlines.

Simulated Experiments

Table 2: The Quantitative Comparison of Different Methods on the dataset Washington DC Mall.

Case	Indicators	Noise	FORPDN	SNLRSF	SSTV-LRTF	LRTDTV	3DTNN	3DLog-TNN	FRCTR-PnP
Case 1	MPSNR	20.001	34.057	**40.029**	35.505	36.720	35.832	37.532	38.168
	MSSIM	0.4018	0.9302	**0.9812**	0.9499	0.9550	0.9646	0.9688	0.9738
	SAM	30.695	6.8732	**2.5679**	4.8184	4.5197	3.8600	3.5857	3.1812
Case 2	MPSNR	10.823	22.231	33.351	33.717	34.934	33.195	35.613	**36.021**
	MSSIM	0.1024	0.7309	0.9021	0.9280	0.9353	0.9359	0.9557	**0.9592**
	SAM	49.176	12.342	8.1513	5.8205	6.4623	5.4231	4.1690	**3.8865**
Case 3	MPSNR	10.161	21.841	30.181	29.527	30.620	26.052	28.086	**32.207**
	MSSIM	0.0873	0.7110	0.8358	0.8404	0.8639	0.7798	0.8204	**0.9121**
	SAM	51.121	14.008	11.624	7.8388	7.4715	12.797	10.823	**7.3728**
Case 4	MPSNR	10.211	22.079	30.379	30.712	31.551	27.430	29.597	**33.374**
	MSSIM	0.0876	0.7141	0.8370	0.8759	0.8823	0.8310	0.8884	**0.9336**
	SAM	51.364	13.446	10.413	7.5820	7.7430	9.5372	7.2102	**5.8634**
Case 5	MPSNR	10.181	21.929	30.371	28.569	29.428	24.099	26.531	**32.258**
	MSSIM	0.0870	0.7115	0.8342	0.8135	0.8214	0.6720	0.7573	**0.9177**
	SAM	51.252	13.705	11.503	11.183	8.3036	13.535	11.699	**7.2065**

Simulated Experiments

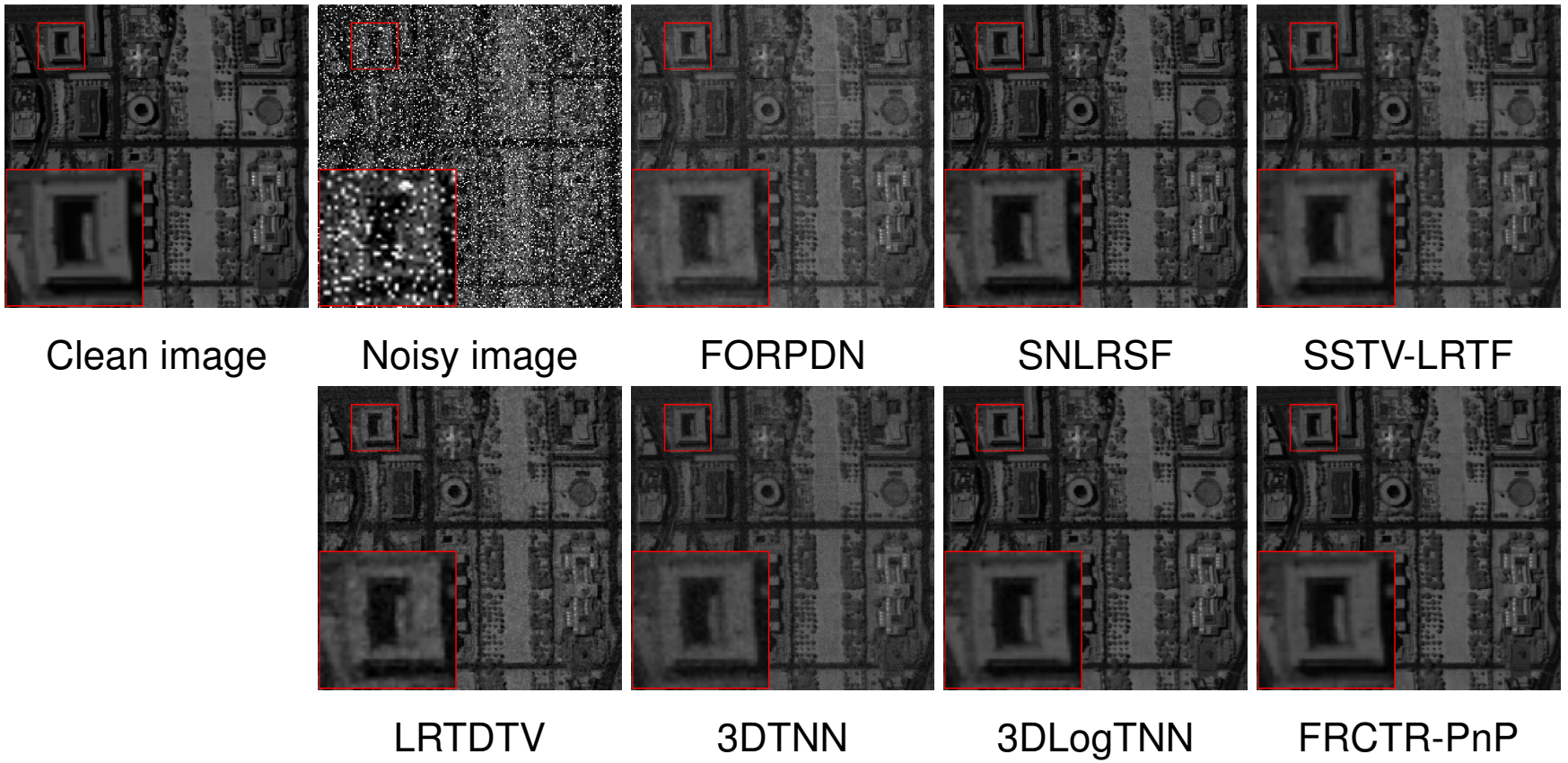

Figure 7: The restored results of band 96 on WDC Mall by different methods for case 2.

Simulated Experiments

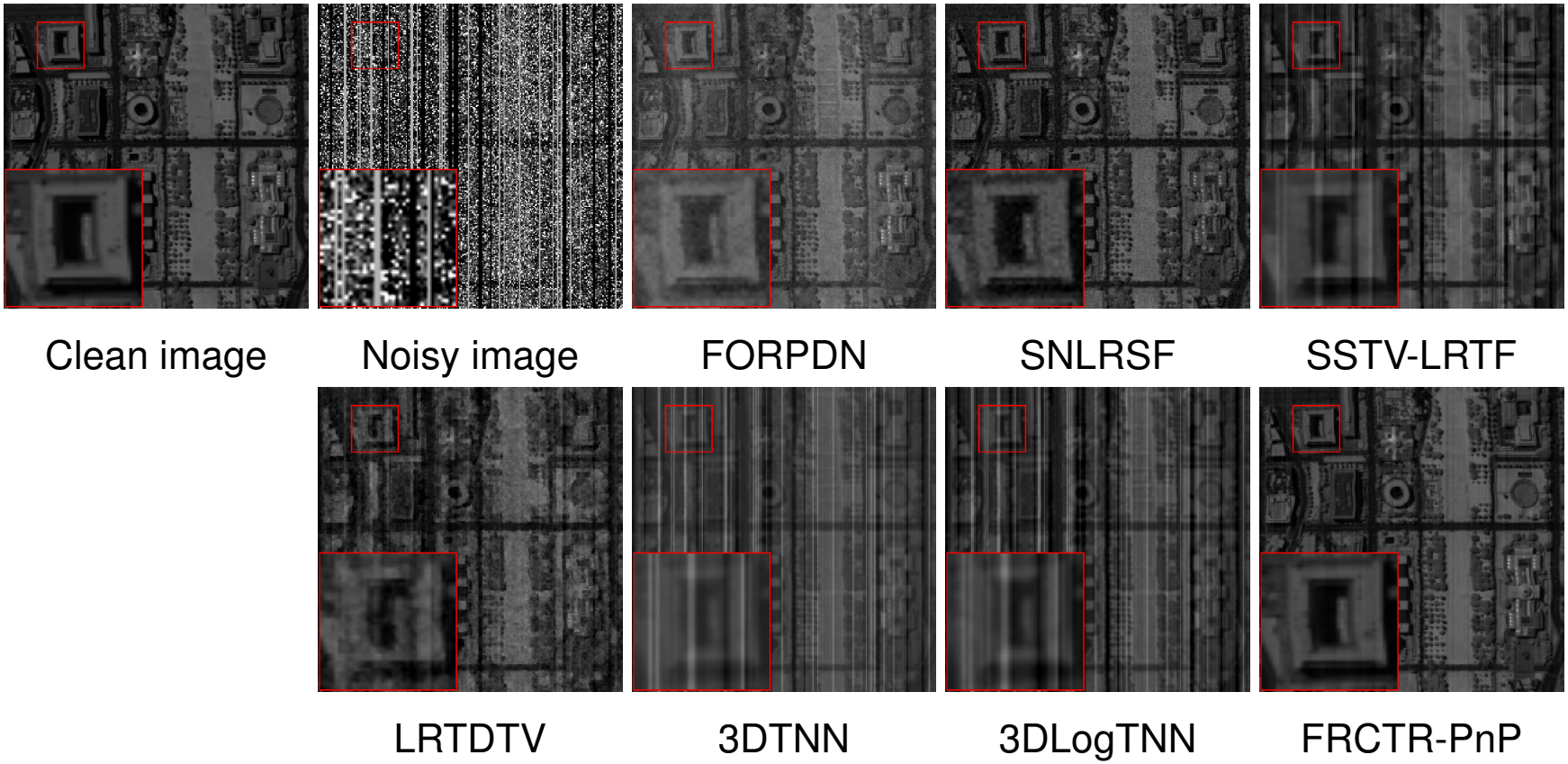

Figure 8: The restored results of band 96 on WDC Mall by different methods for case 5.

Thank you very much for listening!